Preliminary results from the Small Negative Ion Facility (SNIF) at CCFE
J. Zacks, R. McAdams, J. Booth, K. Flinders, A. J. T. Holmes, M Simmonds, B. Stevens, P. Stevenson, E. Surrey, S. Warder, A. Whitehead, and D. Young

Preliminary results from the Small Negative Ion Facility (SNIF) at CCFE

J. Zacks, R. McAdams, J. Booth, K. Flinders, A. J. T. Holmes, M Simmonds, B. Stevens, P. Stevenson, E. Surrey , S. Warder, A. Whitehead, and D. Young

Citation: AIP Conference Proceedings **1515**, 569 (2013); doi: 10.1063/1.4792829
View online: http://dx.doi.org/10.1063/1.4792829
View Table of Contents: http://scitation.aip.org/content/aip/proceeding/aipcp/1515?ver=pdfcov
Published by the AIP Publishing

Preliminary Results From The Small Negative Ion Facility (SNIF) At CCFE

J. Zacks[a], R. McAdams[a], J. Booth[a], K. Flinders[a], A.J.T. Holmes[b], M Simmonds[a], B. Stevens[a], P Stevenson[a], E. Surrey[a], S. Warder[a], A. Whitehead[a], D. Young[a]

[a]*Euratom/CCFE Fusion Association, Culham Science Centre, Abingdon, Oxfordshire, OX14 3DB, UK*
[b]*Marcham Scientific, Hungerford, Berkshire RG17 0LH, UK*

Abstract. At Culham Centre for Fusion Energy, a new beam extraction test facility has been built with the purpose of studying and enhancing negative ion beam production and transport. The multipole hydrogen ion source is based on a RF generated plasma using a continuous 5kW power supply operating at the industrial standard frequency of 13.56MHz. The cylindrical source has a diameter of 30cm and a depth of 20cm, with a flat spiral antenna driving the source through a quartz window. The magnet configuration is arranged to produce a dipole filter field across the ion source close to the plasma grid. The plasma load is matched to the RF generator using a Pi matching network. The accelerator uses a single extraction aperture of 14mm diameter, with a biased insert for electron suppression. The accelerator is a triode design with a beam energy of up to 30kV. The beamline consists of a turbomolecular pumped vacuum tank with an instrumented beam dump and ports for additional diagnostics. The ITER Neutral Beam source operates with the enhancement of caesium, which, when scaled up to a reactor, will be heavily consumed. The small size of SNIF allows for fast turn around of modifications and alternative materials to caesium can be tested. A full description of the facility and planned diagnostics is given. Initial results are presented, including measurements and calculations of the plasma load on the RF generator, and beam extraction measurements.

Keywords: Negative Ion Sources, RF plasma sources, ion beams, ion beam accelerators.
PACS: 41.75.Cn, 52.50.Dg, 52.80.Pi

INTRODUCTION

Hydrogenic neutral beams will be used for heating, current drive and diagnostics on future large magnetic fusion machines such as ITER. Due to the size of the devices and the plasma density, the beam energies required in order to penetrate the plasma are in excess of 1MeV. Due to the neutralisation efficiency being greater than in positive ion beams at these energies, negative ion beams will be used to produce the neutral beams. On ITER [1], each 1MeV heating neutral beam will be obtained from a 40A D^- beam, at an extracted current density of $290Am^{-2}$ to produce 16.7MW of neutral

Third International Symposium on Negative Ions, Beams and Sources (NIBS 2012)
AIP Conf. Proc. 1515, 569-578 (2013); doi: 10.1063/1.4792829
2013 American Institute of Physics 978-0-7354-1136-4/$30.00

beam power. The ITER Neutral Beam source operates with the enhancement of caesium, which, when scaled up to a reactor, may consume as much as 17kg per year [2], and due to its reactivity in air, may create maintenance and storage issues. At CCFE, the Small Negative Ion Facility (SNIF) has been built as a fast turn around test facility capable of testing alternative materials to caesium and studying other enhancement techniques for negative ion production, together with beam transport. This paper presents the facility in sections, starting with the ion source and RF driver, followed by the accelerator and HV power supplies, and then the beamline and diagnostics.

THE SOURCE

Figure 1 shows the main features of the SNIF source and accelerator. The SNIF ion source is a cylindrical source, 30cm in diameter and 20cm deep. The source walls are copper with stainless steel flanges for holding the grids, and an aluminium feedthrough flange at the extraction plane, and a 15cm diameter ceramic window on the backplate, through which the flat spiral RF antenna can couple to the plasma. Feedthroughs were installed on the backplate to allow filaments to be used in the source for aiding plasma breakdown, however these were found to be unnecessary since breakdown was achieved though RF alone.

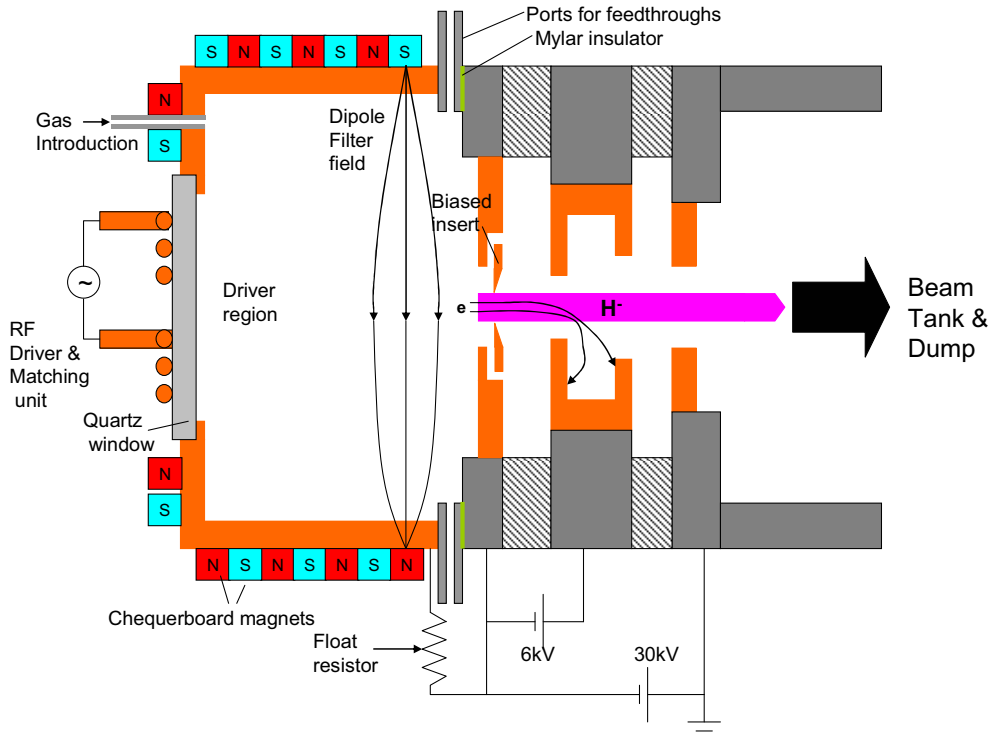

FIGURE 1. The SNIF RF driven, chequerboard source and electron suppressing accelerator.

Initial operation used 10mm thick quartz as the ceramic window. The RF antenna was made of 3.5 turns of 6mm diameter copper tube, with cooling water running through it. Magnets are located on the outside of the source body in a checkerboard arrangement, with a dipole filter field set up near the extraction plane. This dipole field (~2.7Gauss m) allows a region of lower temperature plasma to be created where a greater density of negative ions can be produced.

The source is driven by a 5kW RF generator operating at 13.56MHz. This frequency is an industrial standard, and is an unassigned region of the spectrum, eliminating any risk of stray emission disrupting communications. The generator has an impedance of 50Ω, and is matched to the source using an auto-tuning "Pi" matching network, as shown in figure 2. In this figure, the output load on the matching unit is treated as a resistor and inductor in series. This includes the load of the plasma, the antenna, and the transmission line. A match is achieved through varying the values of the capacitors, C_1 and C_2. These capacitors have ranges of 755-2240pF and 5-250pF respectively. The Pi network inductor was measured to have an inductance of 1.0μH. The unit used also contains capacitors on the output, to act as a DC filter.

Hydrogen flow into the source is controlled by a mass flow controller, located outside the Faraday cage that doubles as the facility's HV enclosure. The achievable range of source pressures has been calculated to be approximately 0.1-1.2Pa, with a normal operating pressure below 0.5Pa. A 5.2cm long ceramic break is used to isolate the source, kept at HV during beam extraction, from the ground potential gas line. The small volume of the source and the high pumping speed meant that careful consideration of the Paschen Curve [3,4] was required so that breakdown across the ceramic was avoided. Expanding the gas line, from 4mm diameter to 12mm diameter at the ceramic break and downstream, allowed the line to enter the low pressure breakdown free regime. Only hydrogen is used in the source, to eliminate the need for shielding, and caesium is not used so as to avoid the associated hazards.

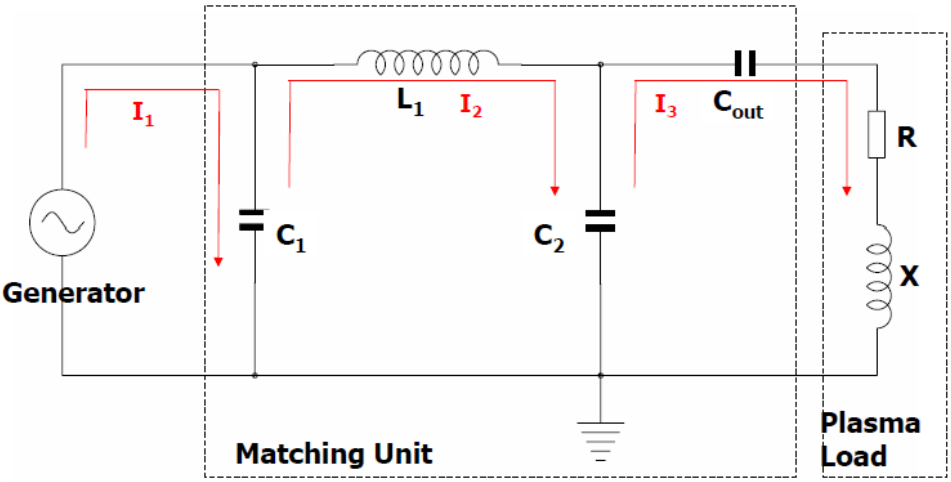

FIGURE 2. Schematic of the "Pi" matching network, and its use in driving the SNIF RF ion source.

During beam extraction, the source body is held at -30kV. However, the RF antenna is kept at earth potential, with the distance between the antenna and ion source body providing sufficient isolation. This was done to reduce losses and make analysis of the RF circuit simpler.

Load Calculations

Treating the load on the matching unit as a resistor and inductor in series with the matching network output, three current loops were setup using Kirchhoff's laws,

$$V = \frac{I_1}{j\omega C_1} - \frac{I_2}{j\omega C_1} \tag{1}$$

$$0 = j\omega L_1 I_2 + \frac{I_2 - I_1}{j\omega C_1} + \frac{I_2 - I_3}{j\omega C_2} \tag{2}$$

$$0 = I_3(R + jX) + \frac{I_3 - I_2}{j\omega C_2} \tag{3}$$

enabling calculation of the resistive (R) and reactive (X) load on the matching unit, through knowledge of the positions of the variable capacitors. These are given in equations 4 and 5.

$$R = \frac{50}{\left[\left(2500(\omega C_1)^2 + 1\right)(\omega C_2)^2\left(\left(\frac{50}{\left[2500(\omega C_1)^2 + 1\right]}\right)^2 + \left(\frac{2500(\omega C_1)}{\left[2500(\omega C_1)^2 + 1\right]} - \omega L_1 + \frac{1}{\omega C_2}\right)^2\right)\right]} \tag{4}$$

$$X = \frac{\omega L_1 - \frac{2500(\omega C_1)}{\left[2500(\omega C_1)^2 + 1\right]} - 1/\omega C_2}{(\omega C_2)^2\left(\left(\frac{50}{\left[2500(\omega C_1)^2 + 1\right]}\right)^2 + \left(\frac{2500(\omega C_1)}{\left[2500(\omega C_1)^2 + 1\right]} - \omega L_1 + \frac{1}{\omega C_2}\right)^2\right)} + \frac{1}{\omega C_2} + \frac{1}{\omega C_{out}} \tag{5}$$

The equation for a lossless transmission line is

$$Z_{in}(l) = Z_0 \frac{\left(Z_L + jZ_0 \tan(\beta l)\right)}{\left(Z_0 + jZ_L \tan(\beta l)\right)} \tag{6}$$

where Z_{in} is the impedance at the start of the line, equal to R+jX, Z_0 is the characteristic impedance of the line (50Ω), Z_L is the load impedance of the plasma and antenna (R_L+jX_L), l is the transmission line length, and β is the RF wave number ($2\pi/\lambda$). This was used, together with the values found from equations 4 and 5, to obtain the resistive and reactive load of the antenna and plasma.

$$R_L = \frac{RZ_0}{A} + Rk\left(XZ_0 - Z_0^2 k + \frac{R^2 k Z_0}{A}\right) \Big/ \left(A^2 + R^2 k^2\right) \tag{7}$$

$$X_L = \left(\frac{XZ_0 - Z_0^2 k}{(Z_0 + kX)} + \frac{R^2 k Z_0}{(Z_0 + kX)^2} \right) \Big/ \left(1 + \frac{R^2 k^2}{(Z_0 + kX)^2} \right) \tag{8}$$

where $k = \tan(\beta l)$ and $A = Z_0 + kX$. Results for the resistance, calculated using equation 7, from a power and gas flow scan, are shown in figure 3.

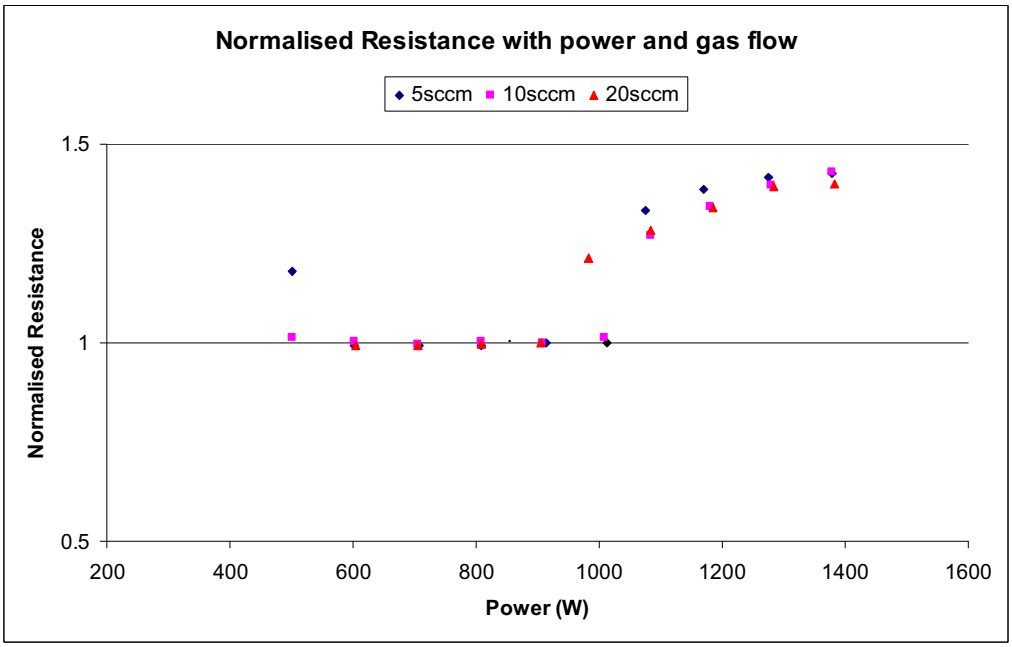

FIGURE 3. Normalised resistance of the antenna and plasma seen for different gas flows and RF input powers.

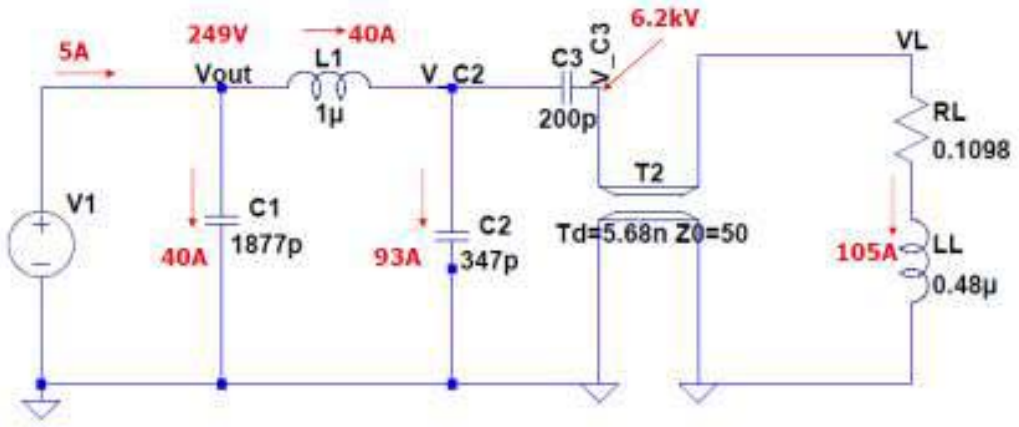

FIGURE 4. Output from LTspice model of SNIF RF circuit operating at 1.2kW.

A transition point is clearly seen in the resistance at the point where the plasma transitions from capacitively coupled to inductively coupled. This transition is also seen visually through the quartz window, by a sudden increase in brightness of the plasma. Reactance calculations show only a shift of 1%.

With the load calculated, the magnitude of voltages and currents at various points in the circuit were also calculated using LTspice software, with results shown in figure 4.

For a 1.2kW plasma, the currents through C_2 and the load were found to be 93A and 105A respectively, with the voltage across the load being 6.3kV. These currents exist despite less than 5A being drawn from the RF power supply, and can push the handling limits of the cables and connectors in the circuit.

Extraction Region Measurements

The plasma grid contains a 63mm diameter biased insert plate, containing the 14mm diameter extraction aperture (area = 1.54cm^2). During extraction, this grid will normally have a positive bias with respect to the anode, allowing a suppression of the electrons co-extracted within the beam. The power supply is rated for 40V and 15A.

A feedthrough flange, 1cm thick is located between the main source body and the plasma grid. As well as being used as a feedthrough for the bias supply connection, this flange allows a dedicated Langmuir probe to be inserted into the plasma in the extraction region. Ports are also available for other diagnostics.

THE ACCELERATOR

The SNIF accelerator is a triode design, capable of producing an H^- beam of energy 30kV, with the plasma grid held at -30kV, and the beamline at earth potential. The grid 1 power supply is rated for 170mA. There is a small resistance (20Ω) between the plasma grid and the source, allowing the source to float with the plasma potential. The grids are copper, with a single beam aperture, and contain a series of neodymium iron boron (NdFeB) magnets to deflect co-extracted electrons on to Grid 2, whilst minimizing deflection of the H^- ions. The extraction grid (Grid 2) is operated at between 2-4kV above the plasma grid, depending on the beam perveance required. The grid 2 power supply is rated for 6kV and 200mA. The highest beam current produced to date is ~3mA (~20Am^{-2}), with a beam voltage of 27kV and RF power of 1.3kW. The grid 2 extraction voltage was set at 3kV, giving a low diversity beam, as expected from the design. This was seen using a visible camera mounted on a port mounted on the top of the vacuum chamber. Current measurement on the grid 2 power supply is limited by a drain current in the water cooling loop. No significant current was seen, though the bias voltage was set to 20V, which is relatively high.

The accelerator design was carried out using the AXCEL Poisson solver for the electric fields, and a particle tracer to combine the effects of both the magnetic and electric fields. A range of current densities were simulated (1-10mAcm^{-2}), across a 2.5-4kV extraction voltage, minimising beam deflection whilst deflecting all co-extracted electrons on to grid 2. Figures 5-7 show simulations of the electron trapping at 2.5kV and 4kV extraction respectively. Figure 8 shows an AXCEL simulation for the 3mA beam obtained, showing a mostly narrow beam with a small halo.

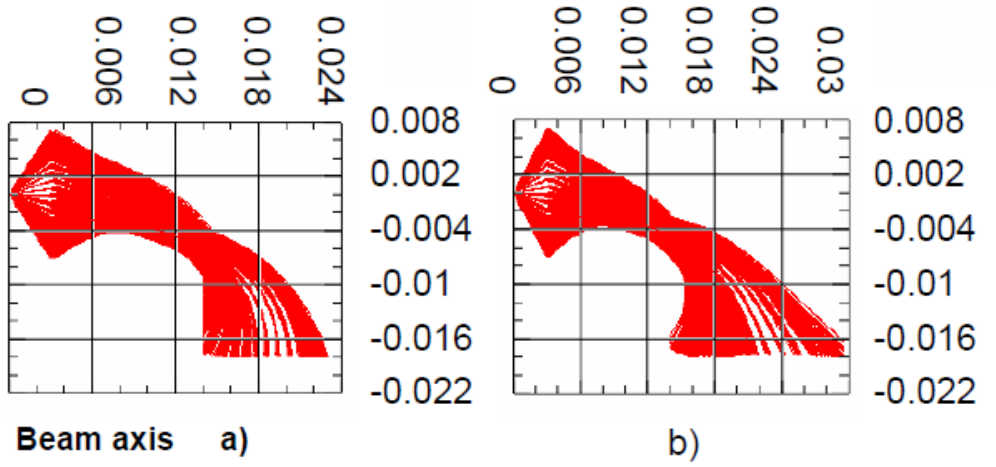

FIGURE 5. Electron trap design simulation for 1mAcm^{-2} at a) 2.5kV and b) 4kV extraction.

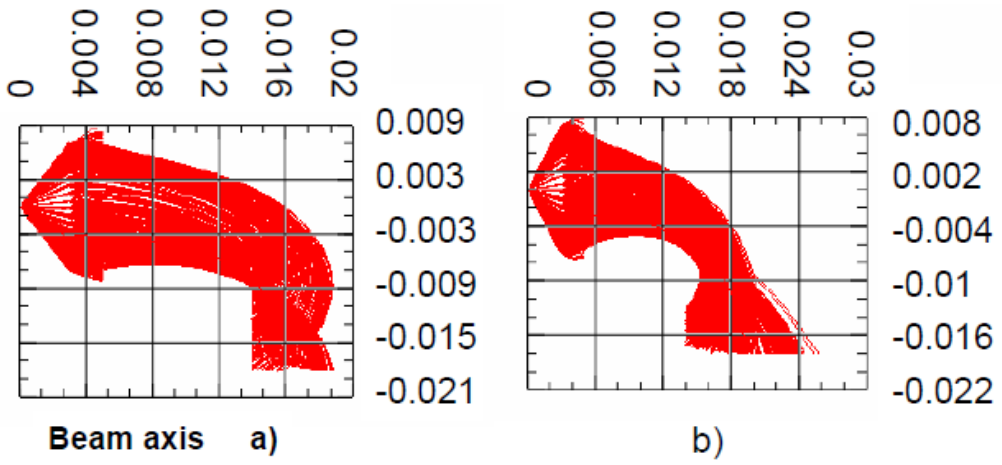

FIGURE 6. Electron trap design simulation for 5mAcm-2 at a) 2.5kV and b) 4kV extraction.

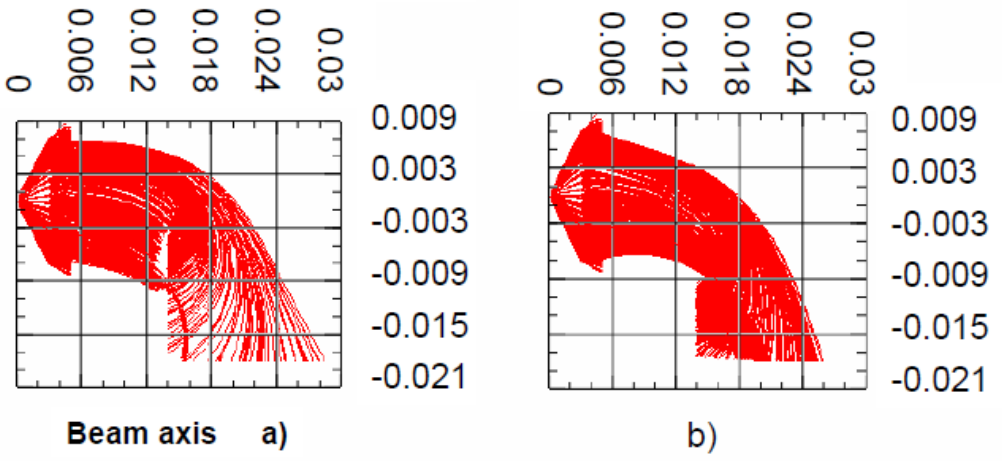

FIGURE 7. Electron trap design simulation for 10mAcm-2 at a) 2.5kV and b) 4kV extraction.

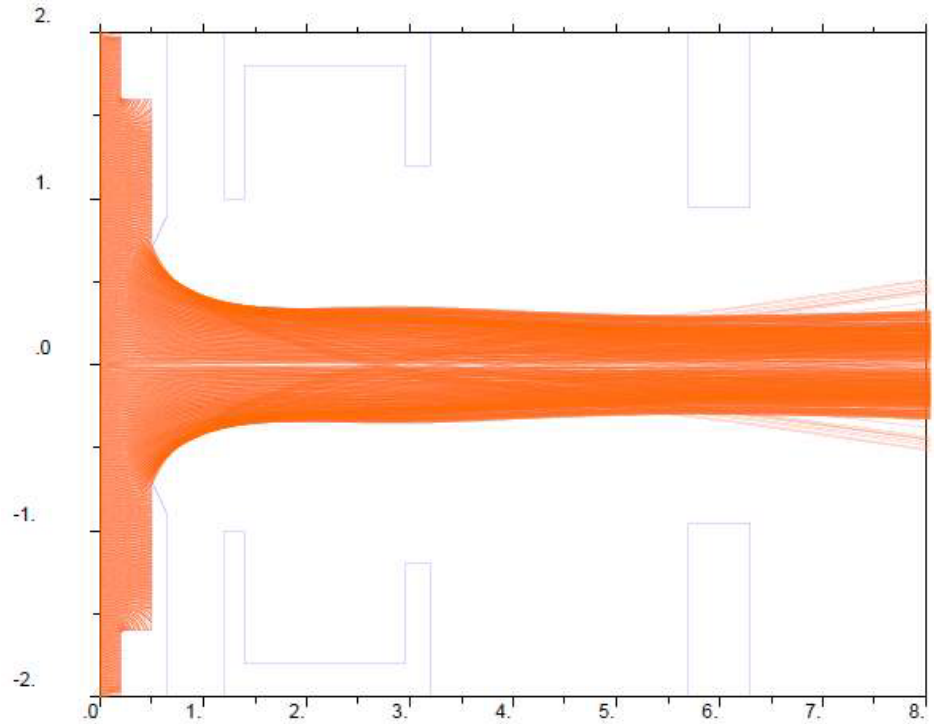

FIGURE 8. AXCEL simulation of 3A SNIF beam at 27kV, with 3kV extraction.

THE BEAMLINE

The SNIF beamline consists of two joined 1000 litre vacuum tanks, with turbo molecular vacuum pumps, which also pump the ion source. At the far end of the beam line is a cooled copper beam dump, instrumented with over 100 thermocouples, creating a grid with 5mm by 5mm resolution which will enable good beam profile measurement. The thermocouples are connected to a fast data acquisition system, capable of taking data at 500kHz. Ports on the vacuum tank provide access for further diagnostics, such as visible cameras, which will enable a good view of the beam profile.

One such diagnostic is a beam profile viewing camera with a narrowband filter for H_α emission. This simple system provides a second method of measuring the beam profile, through its Doppler shifted emission of the H_α line.

A McPherson model 209, 1.33m focal length spectrometer is available to take measurements from the source, as well as the beam. With an Andor Newton CCD detector, the spectrometer is capable of a resolution of 0.007nm and has a range of 300-700nm, allowing use for density measurements, Doppler spectroscopy using the Balmer series, and viewing of the molecular lines associated with the precursors required for volume negative ion production.

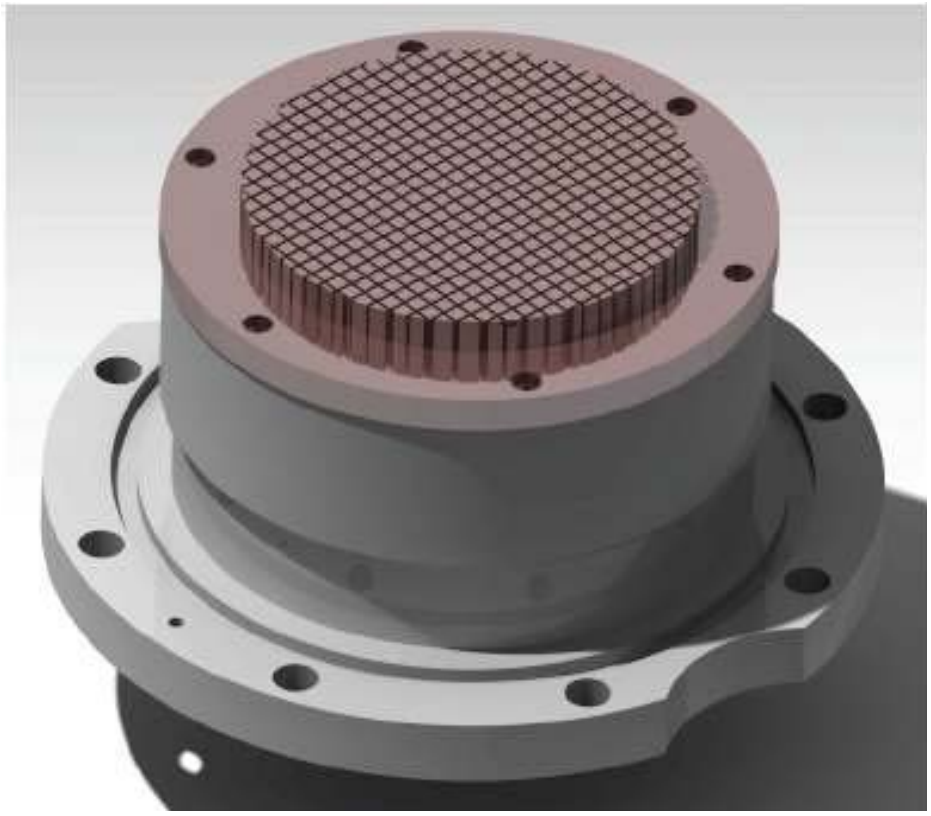

FIGURE 9. CAD rendering of the SNIF copper beam target.

FACILITY OVERVIEW AND DEVELOPMENT PLAN

Due to its small size, modifications can be simple, quick and do not require lifting equipment, allowing a fast turnaround. This is aided by a vacuum pump-down time of less than 3 hours to reach a good operating pressure of 10^{-6}mBar. Future work will make use of this to test different materials as alternatives to caesium, looking for any enhancement of H^- production. Using hydrogen eliminates radiological hazards that would also be an obstacle for making quick modifications.

The HV power supplies on SNIF are both reversible, allowing a positive ion beam to also be produced. This may be used for power load testing by replacing the beam target with test materials.

As well as investigating negative ion production, SNIF will also continue studies of RF coupling, with an alumina ceramic window as an alternative to the quartz, as well as different antenna configurations. Different matching networks may also be used.

Other areas of interest for study include neutraliser development [5], space charge neutralization, beam transport, low pressure operation and electron trapping.

REFERENCES

1. ITER Design Description Document 5.3, N53 DDD 29 01-07-03 R0.1 2003 IAEA, Vienna.
2. E. Surrey, Fusion Engineering and Design 87 (2012) 373– 383.
3. Paschen, F.,Annalen der Physik, vol. 273, Issue 5, pp.69-96.
4. Lieberman and Lichtenberg, Principles of Plasma Discharges, Wiley 2005.
5. E. Surrey, these proceedings.